行政院國家科學委員會專題研究計畫成果報告

非共點控制撓性機械臂之最小相位化研究
Achieving Minimum Phase Behavior for Noncollocated Flexible Manipulators

計畫編號：NSC 88-2212-E-002-010
執行期限：87年8月1日至88年7月31日
主持人：袁　京　　國立台灣大學機械系

一、中文摘要

本計畫就端點具負載之單桿撓性機械臂之完整線性分佈參數模式，選擇適當之虛擬輸出，找出系統在非共點控制下為最小相位之充要條件。也證明了在此充要條件下，系統之無限維零動態並無右半平面之特徵值。由於最小相位僅是系統為passive之必要條件，本計畫更進而發現非passive之最小相位系統可藉由撓性臂根部之應變回授轉換成passive系統。如此則簡單之關節PD控制配合應變回授即可達成虛擬輸出之全程無誤差追蹤，同時也兼具消除振動之能力。由於虛擬輸出已儘量逼近撓性臂端點運動時之實際位置，故可達成撓性機械臂端點之高精確度軌跡追蹤。實例之數值模擬驗證了前述控制方法之優越性。

關鍵詞：撓性機械臂、非共點控制、最小相位化研究

Abstract

A single-link flexible manipulator having a tip payload and with noncollocated actuator and sensor is investigated using a linear distributed parameter model. With the joint torque as the input and the joint angle plus a weighted value of tip deflection as the measured output (called the virtual output), a necessary and sufficient condition in terms of the weighting factor of tip deflection is obtained such that the transfer function of the flexible system does not have any open right-half plane zeros. The equivalence of the zeros of the transfer function and the eigenvalues of the infinite-dimensional zero-dynamics is also verified. It is well known that a minimum phase system needs not be passive. Fortunately, the single-link flexible system can always be made passive by using the strain feedback. This is a remarkable discovery as it makes the exact tracking of the virtual output achievable using simple joint PD control in conjunction with the feedback of root strain of the flexible link. Since the virtual output is closely related to the actual motion of the tip, accurate tracking of the tip of the flexible link can be obtained. The efficacy of the proposed approach is verified by numerical simulation.

Keywords: Flexible manipulator, Noncollocated control, Achieving minimal phase beliavior

二、緣由與目的

對單桿之撓性機械臂而言，若輸入為關節扭矩而輸出為撓性臂端點之位置，則此系統之轉移函數必有右半平面零點，或描述此系統之非線性動態模式具有不穩定之零動態。此種非共點控制在理論上將使輸出之無誤差追縱變成完全不可能[1]。為克服非共點控制所造成之非最小相位的難題，有些研究者利用變更致動器的位置[2]或變更致動器及量測器之位置[3]，希望找

出達成最小相位的條件，結果發現最小相位僅在共點控制下才能達成。另有部分研究者則選擇撓性臂端點以外的點作為輸出[4]－[7]，利用有限維之動態模式找出了一些達成最小相位的條件。惟撓性臂並非有限維系統，文獻[8]發現所有過去文獻中處理之非共點控制，在無限維動態模式下皆仍為非最小相位系統。最近文獻[9]利用撓性臂之線性分佈參數模式，選擇特定之虛擬輸出，首度證實無限維之單桿撓性臂在非共點控制下仍有可能為最小相位。惟文獻[9]採用了過於簡化的無限維動態模式，所選擇之虛擬輸出也不具明確的物理意義，也未找出系統為最小相位之充要條件，更未探討系統是否可為passive的可能性。

本計畫之目的為針對具有端點負載之單桿撓性機械臂，選擇物理意義明確之虛擬輸出，找出此一無限維系統在非共點控制下為最小相位之充要條件。為達成撓性臂端點具備精確且快速之軌跡追蹤能力，吾人希望此一最小相位系統同時也是passive系統。如此則可突破目前文獻中撓性機械臂在控制上所遭遇的主要瓶頸。

三、結果與討論

1.本計畫利用文獻[10]中所提供之包含端點負載單桿撓性機械臂無限維動態模式，選擇關節角及加權後端點變形量之和為虛擬輸出，推導出系統在非共點控制下為最小相位之充要條件。同時也澄清了最近文獻中有關無限維零動態穩定性分析方面的一些盲點[8,9]，此部份之研究成果已投稿送審中（詳見附件）。

2.由於非共點控制下最小相位的單桿撓性臂系統不必然為passive，本計畫進而發現利用應變及剪應力回授可將非passive之最小相位系統轉換成passive系統。如此則簡單的關節PD控制配合應變回授即可達成虛擬輸出之全程無誤差追蹤，同時也兼具消除振動之能力。實例之數值模擬驗了前述控制方法之優越性。此部分之研究成果目前正在撰寫準備投稿中。

四、計畫成果自評

1.本計畫首度就無限維之單桿撓性機械臂系統在非共點控制下找出了系統為最小相位的充要條件。此一問題為撓性機械臂控制領域中長期以來懸而未決的難題。本計畫在這部分的研究成果應可視為相關文獻中的一個重要突破。

2.本計畫首度就無限維之單桿撓性機械臂系統在非共點控制下之無限維零動態的穩定性進行了正確的分析。並指出了目前文獻中所提供方法之缺失。無限維零動態的穩定性問題對於採用非線性控制方法而言，具有關鍵性的重要性。

3.本計畫首度發現了應變及剪應力回授可將非passive之最小相位撓性系統換成passive系統。此一新發現不但進一步瞭解了應變回授在撓性系統控制中之關鍵性作用，更對一些新進發展的控制理論的應用排除了主要障礙。在撓性機械臂的控制領域中，也應視為一個重要的突破。

4.由於本計畫的困難度遠較預期為高，且在研究過程中意外發現了應變回授具有前所未知的功能與意義，因此局部調整了原計畫書之工作項目，處理了一些更重要的關鍵性問題。本計畫之研究成果在相關領域中已作出了非常重要的貢獻。

五、參考文獻

[1] Spector, V.A. and H. Flashner, "Modeling and Design Implications of Noncollocated Control in Flexible Systems," *ASME J. Dyn. Syst. Meas. Contr.*, Vol. 112, pp. 186-193 (1990).

[2] Park, J.H. and H. Asada, "Dynamic Analysis of Noncollocated Flexible Arms and Design of Torque Transmission Mechanisms," *ASME J. Syst. Meas. Contr.*, Vol. 116, pp. 201-207 (1994).

[3] De Luca, A. and L. Lanari. "Achieving Minimum Phase Behavior in a One-Link Flexible Arm," *Proc, Int. Symp. on*

Intelligent Robotics, Bangalore, India, pp. 224-235 (1991).

[4] De Luca, A., P. Lucibello, and G. Ulivi, "Inversion Techniques for Trajectory Control of Flexible Robot Arms," *J. Rob. Syst.*, Vol. 6, pp. 325-344 (1989).

[5] De Luca, A., "Zero Dynamics in Robotic Systems," in Nonlinear Synthesis (C.I. Byrnes and A. Kurzhansky, Eds.), Birkhauser, Boston, pp. 68-87 (1991).

[6] Madhavan, S.K., and S.N. Singh, "Inverse Trajectory Control and Zero Dynamics Sensitivity of an Elastic Manipulator," *Proc. 1991 American Contr. Conf.*, Boston, MA., pp. 1879-1884 (1991).

[7] Wang, D. and M. Vidyasagar, "Transfer Function for a Single Flexible Link," *Int. J. Robot. Res.*, Vol. 10, pp. 540-549 (1991).

[8] Tarn, T.J., C. Guo and A.K. Bejczy, "Issues in the Zeros of Flexible Robot Systems." *Proc. 32nd Allerton Conf. on Communication, Control and Computing*, pp. 641-650 (1994).

[9] Chodavarapu, P.A. and M.W. Spong, "On Noncollocated Control of a Single Flexible Link," *Proc. IEEE Int. Conf. on Rob. Autom.*, Minneapolis, Minnesota, pp. 1101-1106 (1996).

[10] Lee, S. and J.L. Junkins, "Explicit Generalization of Lagrange's Equations for Hybrid Coordinate Dynamical systems," *J. Guid., Contr., and Dyn.*, Vol. 15, pp. 1443-1452 (1992).

國科會研究報告(NSC88-2212-E-002-010)

ACHIEVING MINIMUM PHASE TRANSFER FUNCTION FOR A NONCOLLOCATED SINGLE-LINK FLEXIBLE MANIPULATOR

King Yuan and Liang-Yih Liu

ABSTRACT

A noncollocated system has the potential of providing more precise tracking, improved disturbance rejection and increased bandwidth at the sensor location, but is considerably more difficult to stabilize than a collocated system due to its nonminimum phase nature. For a flexible manipulator, the problem becomes even more complicated because the system is inherently infinite dimensional. In this paper, a single-link flexible manipulator having a tip payload and with noncollocated actuator and sensor is investigated using a linear distributed parameter model. With the joint torque as the input and the joint angle plus a weighted value of tip deflection as the measured output, an exact transfer function involving transcendental functions is derived. Using the methods of infinite product expansion, root locus, and asymptotic property of roots of transcendental equation, a necessary and sufficient condition in terms of the weighting factor of tip deflection is obtained such that the transfer function does not have any open right-half plane zeros. This condition depends neither on the physical properties of the link nor on the mass properties of the tip payload. In order to clarify the misinterpretation appeared in some closely-related works concerning the stability issue of the infinite-dimensional zero-dynamics, the equivalence of the zeros of the transfer function and the eigenvalues of zero-dynamics is also verified.

Keywords: Flexible manipulator, distributed parameter model, noncollocated control, minimum phase system.

*The authors are with Dept. of Mechanical Engineering, National Taiwan University, Taipei, Taiwan, R.O.C.
Tel: 886-2-23913694
Fax: 886-2-23913694
E-mail: ky260112@ms16.hinet.net

**This work was supported by National Science Council of R.O.C. under grant NSC 88-2212-E-002-010.

I. INTRODUCTION

In noncollocated control of a single-link flexible manipulator, the presence of open right half-plane zeros in the transfer function relating the joint torque to the tip position has long been recognized as the source of performance limitation due to the nonminimum phase nature of the open-loop system [1, 2]. To cope with this difficulty, two approaches have been proposed in the literature. The first approach involves the relocation of torque actuation by a torque transmission mechanism [3]. Despite their complicated mechanical structure of the flexible arm, a minimum phase system can be attained in [3] only when the actuator and sensor are completely collocated at the tip point of the flexible link. Moreover, the conclusion was reached in [3] based on a finite-dimensional model without taking full account of the mass properties of the hub and tip payload. A similar approach which considers the relocations of both the torque actuation point and the output measurement point along the link was studied in [4] using a finite-dimensional model. Unfortunately, as the number of modes in the dynamic model increases, a minimum phase system is achieved still with the collocated situations.

The second approach is to use an output other than the actual tip position of the flexible link. These include the angular position of a point located on the link [5], the joint angle plus a weighted value of tip deflection [6, 7], the reflected tip position

[8], the projection of the tip point on a rotating rigid axis [9], and the joint angle augmented with a weighted value of the slope of the link at its tip [10]. Among all these works, with the exception of [9, 10], the stability of zero dynamics was studied relying on approximate finite-dimensional models. An important drawback of this finite-dimensional approach is that the stability of the inherently infinite-dimensional zero dynamics can never be ensured. Stated differently, it is impossible to find the minimum phase condition of a flexible system using finite-dimensional models. For example, the analysis performed by Spector and Flasher [2] using an infinite-dimensional model clearly rejects the validity of the results obtained in [5] based on an approximate finite-dimesional model. Therefore, in order to establish the necessary and sufficient condition for a noncollocated single-link flexible manipulator to be minimum phase, there is no alternative but to resort to an accurate infinite-dimensional model of the flexible link.

As for the single-link flexible manipulator without a tip payload, Tarn et al. [9] have shown based on a linear infinite-dimensional model that all noncollocated outputs considered in prior literature have led to unstable zero dynamics. To remedy this difficulty, Chodavarapu and Spong [10] have recently proposed a virtual angle of rotation as the noncollocated output. With this output, they showed that the transfer function does not have any zeros in the open right half-plane, but failed to establish the relation between the zero-dynamics and the zeros of the transfer

function. It is noteworthy to remark that the methodology used in [9, 10] to search for the zero-dynamics characterizes only the real positive eigenvalues of the zero dynamics, leaving the zeros with unstable complex eigenvalues completely ignored. Therefore their method cannot be used to establish the necessary and sufficient condition for a noncollocated single-link flexible manipulator system to be minimum phase, nor can it be used to establish the relation between the zero-dynamics and the zeros of the transfer function. Although it is well known that [11], for a finite-dimensional linear constant system, the eigenvalues of zero-dynamics and the zeros of the transfer function are equivalent, its counterpart for an infinite-dimensional model of the single-link flexible manipulator does not seem to exist in the existing literature.

In this paper, an infinite-dimensional model of the single-link flexible manipulator with a tip payload is considered. The input is the joint torque. The joint angle plus a weighted value of tip deflection originally suggested in [6, 7] is chosen as the noncollocated output. Thanks to the root locus method, we are able to derive a necessary and sufficient condition such that the transfer function of the single-link flexible manipulator system does not have any open right-half plane zeros. With the help of the well-known formulation of linear eigenvalue problem, we can further establish the equivalence of eigenvalues of zero-dynamics and the zeros of the transfer function.

The organization of the paper is as follows. Section II presents the mathematical model considered, emphasizing the relation between the clamped and pinned conditions at the joint. The transfer function involving transcendental functions is derived in Section III. In Section IV the infinite product expansions of transcendental functions and the root locus method are used to establish the condition for the nonexistence of right half-plane zeros. The equivalence of the spectrum of zero-dynamics and the zeros of the transfer function is shown in Section V. Some conclusions are summarized in Section VI.

II. MATHEMATICAL MODEL

Consider the single link flexible manipulator shown in Fig. 1, moving on a horizontal plane. The link is assumed to be a uniform, homogeneous, Euler-Bernoulli beam of length ℓ, mass per unit length ρ, and flexural rigidity EI. The hub is modelled by a single-mass moment of inertia I_h, where the driving torque $\tau(t)$ is applied. The payload has a mass m_p and the mass moment of inertia J_p. Also shown in Fig. 1, $\theta(t)$ designates the hub rotation angle, and $v(x,t)$ denotes the small elastic deflection of the link. The equatons of motion and its corresponding boundary conditions are well-established (e.g. [12]):

$$I_h\ddot{\theta}(t)+\int_0^{\ell}\rho x[x\ddot{\theta}(t)+\ddot{v}(x,t)]dx+m_p\ell[\ell\ddot{\theta}(t)+\ddot{v}(\ell,t)]$$

$$+J_p[\ddot{\theta}(t)+\ddot{v}_x(\ell,t)]=\tau(t), \tag{1}$$

$$\rho[x\ddot{\theta}(t)+\ddot{v}(x,t)]+EIv_{xxxx}(x,t)=0, \tag{2}$$

$$v(0,t)=0, \tag{3}$$

$$v_x(0,t)=0, \tag{4}$$

$$m_p[\ell\ddot{\theta}(t)+\ddot{v}(\ell,t)]-EIv_{xxx}(\ell,t)=0, \tag{5}$$

$$J_p[\ddot{\theta}(t)+\ddot{v}_x(\ell,t)]+EIv_{xx}(\ell,t)=0, \tag{6}$$

where $(\dot{})$ and $(\quad)_x$ denote $\frac{\partial}{\partial t}$ and $\frac{\partial}{\partial x}$ respectively. Substituting (2)-(6) into (1) yields

$$I_h\ddot{\theta}(t)=\tau(t)+EIv_{xx}(0,t). \tag{1'}$$

Introducing the new variable $w(x,t)$ such that

$$w(x,t)=x\theta(t)+v(x,t), \tag{7}$$

then the clamped-end equations (1'), (2)-(6) reduce to the commonly used pinned-end equations:

$$\rho\ddot{w}(x,t)+EIw_{xxxx}(x,t)=0, \tag{8}$$

$$w(0,t)=0, \tag{9}$$

$$w_x(0,t) = \theta(t), \tag{10}$$

$$m_p \ddot{w}(\ell,t) - EIw_{xxx}(\ell,t) = 0, \tag{11}$$

$$J_p \ddot{w}_x(\ell,t) + EIw_{xx}(\ell,t) = 0, \tag{12}$$

$$I_h \ddot{\theta}(t) = \tau(t) + EIw_{xx}(0,t). \tag{13}$$

III. TRANSFER FUNCTION WITH NONCOLLOCATED INPUT AND OUTPUT

Let the output be chosen as

$$y(t,k) = \ell\theta(t) + kv(\ell,t), \tag{14}$$

where k is a real parameter whose permissible values will be determined to satisfy the minimum phase condition. Note that (14) includes the joint angle output $(k=0)$, the tip position output $(k=1)$, and the reflected tip position output $(k=-1)$ as special cases. Clearly, (14) is more physically appealing than $y(t,k) = \theta(t) + kv_x(\ell,t)$, the one proposed by Chodavarapu and Spong [10]. To express $y(t,k)$ in terms of $w(x,t)$, we have

$$y(t,k) = (1-k)\ell\theta(t) + kw(\ell,t). \tag{15}$$

The transfer function can now be derived by taking Laplace transform of (8)-(14) with zero initial conditions. Let s be the Laplace transform variable, and define

the following dimensionless parameters

$$\beta^4 = -\frac{\rho \ell^4}{EI} s^2 = -\hat{s}^2, \tag{16}$$

$$m_p^* = \frac{m_p}{\rho \ell}, \tag{17}$$

$$J_p^* = \frac{J_p}{\rho \ell^3}. \tag{18}$$

After tedious algebraic manipulations, we obtain

$$G(s,k) = \frac{y(s,k)}{\tau(s)} = \frac{\ell^2}{\beta} \cdot \frac{\beta K_2(\beta) + k K_3(\beta)}{EI\beta K_1(\beta) + I_h s^2 \ell K_2(\beta)}, \tag{19}$$

where

$$\begin{aligned} K_1(\beta) &= \sinh\beta\cos\beta - \cosh\beta\sin\beta \\ &\quad - 2m_p^*\beta\sinh\beta\sin\beta - 2J_p^*\beta^3\cosh\beta\cos\beta \\ &\quad - m_p^* J_p^* \beta^4(\sinh\beta\cos\beta - \cosh\beta\sin\beta), \end{aligned} \tag{20}$$

$$\begin{aligned} K_2(\beta) &= 1 + \cosh\beta\cos\beta - m_p^*\beta(\cosh\beta\sin\beta - \sinh\beta\cos\beta) \\ &\quad - J_p^*\beta^3(\cosh\beta\sin\beta + \sinh\beta\cos\beta) \\ &\quad - m_p^* J_p^* \beta^4(\cosh\beta\cos\beta - 1), \end{aligned} \tag{21}$$

$$\begin{aligned} K_3(\beta) &= \sinh\beta + \sin\beta - \beta(1 + \cosh\beta\cos\beta) \\ &\quad + m_p^*\beta^2(\cosh\beta\sin\beta - \sinh\beta\cos\beta) \\ &\quad - J_p^*\beta^3[\cosh\beta - \cos\beta - \beta(\cosh\beta\sin\beta + \sinh\beta\cos\beta)] \\ &\quad + m_p^* J_p^* \beta^5(\cosh\beta\cos\beta - 1). \end{aligned} \tag{22}$$

Note that the poles of $G(s,k)$, which are independent of k, denote the natural frequencies (including the rigid-body modes) of the flexible system. The computation of these natural frequencies and their experimental verification can be found, for example, in [13, 14, 15]. Our objective in the next section is to find the range of values of k such that the zeros of $G(s,k)$ lie completely on the imaginary axis in the s-plane, irrespective of the values of m_p^* and J_p^*. Toward this end, the infinite product expansions [16] of transcendental functions involved in $K_2(\beta)$ and $K_3(\beta)$ are particularly useful, and are summarized in the Appendix for reference. The convergence of such infinite product expansions is assured by the Mittag-Leffler theorem [17].

IV. CONDITION FOR THE NONEXISTENCE OF RIGHT HALF-PLANE ZEROS

For convenience, the numerator of $G(s,k)$ can be rewritten as

$$Z(\beta,k,m_p^*,J_p^*) = Z_1(\beta,k) + m_p^* Z_2(\beta,k) + J_p^* Z_3(\beta,k) + m_p^* J_p^* Z_4(\beta,k), \tag{23}$$

where

$$Z_1(\beta,k) = (1-k)\beta(1+\cosh\beta\cos\beta) + k(\sinh\beta+\sin\beta), \tag{24}$$

$$Z_2(\beta,k) = (1-k)\beta^2(\sinh\beta\cos\beta - \cosh\beta\sin\beta), \tag{25}$$

$$Z_3(\beta,k) = -\beta^3[(1-k)\beta(\cosh\beta\sin\beta+\sinh\beta\cos\beta) + k(\cosh\beta-\cos\beta)], \tag{26}$$

$$Z_4(\beta,k) = -(1-k)\beta^5(\cosh\beta\cos\beta - 1). \tag{27}$$

In what follows, the root locus method will be applied consecutively to find the range of values of k such that the roots of each of the transcendental equations $Z_1(\beta,k) = 0$, $Z_1(\beta,k) + m_p^* Z_2(\beta,k) = 0$, $Z_1(\beta,k) + J_p^* Z_3(\beta,k) = 0$, and $Z(\beta,k,m_p^*,J_p^*) = 0$ lie completely on the imaginary axis in the s-plane. Note that each of the above equations can be transformed to the $\hat{s}$-plane by (16), i.e. $\beta = \pm(1\pm j)\sqrt{\frac{\hat{s}}{2}}$. If $\hat{s} = \pm j\omega$, there ω is a real positive constant, then β must be $\pm\sqrt{\omega}$ and $\pm j\sqrt{\omega}$. Note further that if $\beta = \sqrt{\omega}$ is a root of any of the above equations, then so are $-\sqrt{\omega}$ and $\pm j\sqrt{\omega}$. Therefore, in order for any of the above transcendental equations to have root on the imaginary $\hat{s}$-axis, it suffices only to search for the real positive roots β of that equation.

Case 1. $Z_1(\beta,k) = 0$ **(*i.e.* $m_p^* = J_p^* = 0$)**

In this case, the zeros of $G(s,k)$ are given by the roots of

$$\frac{k}{1-k}\cdot\frac{\prod_{n=1}^{\infty}\left[1-\frac{\hat{s}^2}{\omega_{zn}^2}\right]}{\prod_{m=1}^{\infty}\left[1+\frac{\hat{s}^2}{\omega_{pm}^2}\right]} = -1, \tag{28}$$

where A1 and A2 from the Appendix have been used in deriving (28). Note that ω_{pm} are the well-known clamped-free bending vibration modes. The lowest 6

modes of ω_{zn} and ω_{pm} are listed in Table 1. The root locus of (28) for $-\infty < k < 1$ is shown in Fig. 2 based on a 6 pole-zero pair approximation. The approximate breakaway points on the imaginary $\hat{s}$-axis are $\pm 12.20j$, $\pm 92.10j$, $\pm 260.66j$ corresponding to $k =$ 0.759, 0.918, 0.984, respectively. Note that the breakaway points on the imaginary $\hat{s}$-axis actually corresponds to the real positive double roots of $Z_1(\beta, k) = 0$, or equivalently,

$$\cosh\beta\cos\beta = -1 - \frac{k}{1-k}\frac{1}{\beta}(\sinh\beta + \sin\beta). \tag{29}$$

Further, the asymptotic behavior of (29) is governed by

$$\beta\cos\beta = -\frac{k}{1-k}. \tag{30}$$

It is easy to verify from the numerical solutions of (29) and simple graph of (30) that (i) the smallest real positive double roots $\beta = 3.483$ $(\hat{s} = \pm 12.132j)$ occur when $k = 0.758$, (ii) a larger value of real positive double roots occur at a larger value of k, and (iii) there are no real positive double roots for $k < 0.758$. Therefore it is impossible to have any breakaway point on the imaginary $\hat{s}$-axis for $k < 0.758$. We conclude that, with the previously defined input and output, the single-link flexible manipulator without a tip payload is minimum phase iff $-\infty < k \leq 0.758$. We emphasize here that this necessary and sufficient condition is obtained via the numerical solution of the exact transcendental equation $Z_1(\beta, k) = 0$, not by the

finite-dimensional approximation of the root locus.

Case 2. $Z_1(\beta,k)+m_p^*Z_2(\beta,k)=0$ (i.e. $m_p^*>0,\ J_p^*=0$)

Let $\hat{s}=\pm j\omega_{\alpha m}(k)$ denote the imaginary roots resulting from $Z_1(\beta,k)=0$ for $k\le 0.758$. Using the infinite product expansion method [2] to express $Z_1(\beta,k)$ and replacing $Z_2(\beta,k)$ by the expression A3, the zeros of $G(s,k)$ are given by the roots of

$$\frac{1}{3}m_p^*(1-k)\frac{\hat{s}^2\prod_{n=1}^{\infty}\left[1+\frac{\hat{s}^2}{\omega_{\beta n}^2}\right]}{\prod_{m=1}^{\infty}\left[1+\frac{\hat{s}^2}{\omega_{\alpha m}^2(k)}\right]}=-1, \tag{31}$$

where $\omega_{\beta n}$ are the familar pinned-free bending vibration modes. The lowest 6 modes of $\omega_{\beta n}$ can be found in Table 1. The numerical solutions of $Z_1(\beta,k)=0$ (i.e. $\omega_{\alpha m}(k)$) for several values of k are listed in Table 2. The root locus of (31) for $0<m_p^*<\infty$ is shown in Fig. 3. Recall from Case 1 that $s=\pm j\omega_{\alpha m}(k)$ cannot be a pair of breakaway points for $k<0.758$, and that there exists only one pair of breakaway points $\hat{s}=\pm 12.132j$ for $k=0.758$. It is clear that the imaginary poles of (31) are well separated for $k<0.758$. According to (30) and confining to $\hat{s}=+j\beta^2$, there must exist one and only one pole $\hat{s}=j\omega_{\alpha m}(k)$ with $k<0.758$ in every interval $(m-\frac{5}{8})\pi<\beta<(m-\frac{3}{8})\pi$ for sufficiently large m. Numerical

solutions (see Table 2) reveals that this inequality condition even holds for $m=3$. Note further that the consecutive zeros $\hat{s}=j\omega_{\beta n}$ are specified by $\beta=(n-\frac{3}{4})\pi$ and $\beta=(n+\frac{1}{4})\pi$ for sufficiently large n (see Table 1). Therefore, with the exception of a pair of zeros at the origin, (31) must have alternating imaginary poles and zeros for $n\geq 2$, $m\geq 3$, and $k<0.758$, in accordance with Fig. 3. Because (31) has a pair of zeros at the origin, insofar as $k\leq 0.758$ the root locus for $0\leq m_p^*<\infty$ lie completely on the imaginary $\hat{s}$-axis even though there is a pole-zero flipping ($\omega_{\alpha 2}$ and $\omega_{\beta 1}$) at $k=0.730$. We conclude that the joint-actuated single-link flexible manipulator with a tip mass ($m_t>0$) but negligible tip inertia ($J_p=0$) remains minimum phase for $k\leq 0.758$ if (14) is chosen as the output.

Case 3. $Z_1(\beta,k)+J_p^*Z_3(\beta,k)=0$ (i.e. $m_p^*=0$, $J_p^*>0$)

To find the roots of the above equation, we write

$$J_p^*\frac{Z_3(\beta,k)}{Z_1(\beta,k)}=-1, \tag{32}$$

Using A4 and A5, $Z_3(\beta,k)=0$ can be expressed as

$$\frac{1}{2}\cdot\frac{k}{1-k}\cdot\frac{\prod_{n=1}^{\infty}\left[1-\frac{\hat{s}^2}{4n^4\pi^4}\right]}{\prod_{m=1}^{\infty}\left[1+\frac{\hat{s}^2}{\omega_{zm}^2}\right]}=-1. \tag{33}$$

Note that (33) can be solved similar to Case 1. It is found that the roots of (33) lie completely on the imaginary $\hat{s}$-axis for $k \le 0.849$, and that there exist a pair of breakaway points on the imaginary $\hat{s}$-axis for $k = 0.849$. The numerical solution of $Z_3(\beta,k) = 0$, i.e. $\hat{s} = \pm j\omega_{\gamma n}(h)$, are listed in Table 3 only for $k \le 0.758$ by reason of consistency. Now applying the infinite product expansion method to express $Z_3(\beta,k)$ and $Z_1(\beta,k)$, (32) can be rewritten as

$$\frac{1}{2}J_P^*(2-k)\frac{\hat{s}^2\prod_{n=1}^{\infty}\left[1+\frac{\hat{s}^2}{\omega_{\gamma n}^2(k)}\right]}{\prod_{m=1}^{\infty}\left[1+\frac{\hat{s}^2}{\omega_{\alpha m}^2(k)}\right]} = -1. \tag{34}$$

Recall that for sufficiently large m we have $(m-\frac{5}{8})^2\pi^2 < \omega_{\alpha m}(k) < (m-\frac{3}{8})^2\pi^2$. Further, since the asymptotic behavior of $Z_3(\beta,k) = 0$ is governed by

$$\beta(\sin\beta + \cos\beta) = -\frac{k}{1-k}, \tag{35}$$

there exists one and only one zero $\hat{s} = j\omega_{\gamma n}(k)$ with $k \le 0.758$ in every interval $(n-\frac{1}{8})\pi > \beta > (n-\frac{3}{8})\pi$, or equivalently, $(n-\frac{1}{8})^2\pi^2 > \omega_{\gamma n}(k) > (n-\frac{3}{8})^2\pi^2$ for sufficiently large n. Numerical results (see Table 3) also verify that this inequality condition holds even for $n = 3$. Therefore, with the exception of a pair of zeros at the origin, (34) must have alternating poles and zeros on the imaginary $\hat{s}$-axis for $n \ge 2$, $m \ge 3$, and $k \le 0.758$, in accordance with Fig. 4. From this figure, we see

that the first non-zero zero intersects the first pole as k approaches 0.758. Numerical computation reveals that $\omega_{\eta}(k)$ intersects $\omega_{\alpha_1}(k)$ at $k=0.742$ (see Tables 2 and 3). The pole-zero flipping in the range of $0.742<k<0.758$ will produce breakaway points on the imaginary $\hat{s}$-axis for sufficiently large J_p^*. We conclude that the roots of (34), or equivalently (32), lie completely on the imaginary $\hat{s}$-axis so long as $k \le 0.742$. By comparing the above result with the one-mode analysis performed in [6], we are forced to conclude that the zero dynamics predicted by an over-simplified finite-dimensional model are usually questionable.

Case 4. $Z_1(\beta,k)+m_p^* Z_2(\beta,k)+J_p^* Z_3(\beta,k)+m_p^* J_p^* Z_4(\beta,k)=0$

In this case, the above equation can be recasted as

$$\frac{m_p^* Z_2(\beta,k)+m_p^* J_p^* Z_4(\beta,k)}{Z_1(\beta,k)+J_p^* Z_3(\beta,k)}=-1. \tag{36}$$

In order to find the zeros of (36), we write

$$\frac{1}{4}J_p^* \frac{\hat{s}^2 \prod_{n=1}^{\infty}\left[1+\frac{\hat{s}^2}{\omega_{\delta n}^2}\right]}{\prod_{m=1}^{\infty}\left[1+\frac{\hat{s}^2}{\omega_{\beta m}^2}\right]}=-1, \tag{37}$$

where A3 and A6 have been used to express $Z_2(\beta,k)$ and $Z_4(\beta,k)$. The lowest 6 modes of $\omega_{\delta n}$ and $\omega_{\beta m}$ can be found in Table 1. Note that , besides a pair of

zeros at the origin, (37) has alternating imaginary poles and zeros along the imaginary $\hat{s}$-axis. As a consequence, the roots of (39) must lie on the imaginary $\hat{s}$-axis for all $J_p^* > 0$, independent of k. The root locus of (37) is shown in Fig. 5. Recall also from Case 3 that the poles of (36) are on the imaginary $\hat{s}$-axis for all $J_p^* > 0$ and $k \le 0.742$. Let $\hat{s} = \pm j\omega_{\xi n}(J_p^*)$ and $\hat{s} = \pm j\omega_{\mu m}(J_p^*)$ denote the non-zero imaginary roots of (37) and (34) for $k \le 0.742$, respectively. The infinite product expansion of (36) can be expressed as

$$\frac{1}{3}m_p^*(1-k)\frac{\hat{s}^2\prod_{n=1}^{\infty}\left[1+\frac{\hat{s}^2}{\omega_{\zeta n}^2(J_p^*)}\right]}{\prod_{m=1}^{\infty}\left[1+\frac{\hat{s}^2}{\omega_{\mu m}^2(J_p^*,k)}\right]} = -1. \tag{38}$$

Note that the poles and zeros of (38) are provided by Figs. 4 and 5, respectively. Thus as shown in Fig. 6, there is one pole in each of the shaded strips: $0 \le \mathrm{Im}\,\hat{s} \le \omega_{\alpha_1}$ and $\omega_{\gamma,n-1} \le \mathrm{Im}\,\hat{s} \le \omega_{\alpha n}$ for $n \ge 2$, and there is one zero in each of the dashed rectangular strips: $0 \le \mathrm{Im}\,\hat{s} \le \omega_{\beta_1}$ and $\omega_{\delta,n-1} \le \mathrm{Im}\,\hat{s} \le \omega_{\beta n}$ for $n \ge 2$. Although the pole-strips and zero-strips are interwoven, the root locus of (38) for the limiting cases $J_p^* = 0$ and $J_p^* = \infty$ are straightforward. This is because alternating poles and zeros on the imaginary $\hat{s}$-axis are automatically satisfied as shown by (a) and (c) in Fig. 6. As for the general case $0 < J_p^* < \infty$, interlacing poles and zeros are no longer obvious. However, with the asymptotic properties $(n-\frac{1}{8})^2\pi^2 > \omega_{\gamma n}(k) >$

$(n-\frac{3}{8})^2\pi^2$, $(n-\frac{3}{8})^2\pi^2 > \omega_{\alpha n}(k) > (n-\frac{5}{8})^2\pi^2$, $\omega_{\beta n} = (n+\frac{1}{4})^2\pi^2$, and $\omega_{\delta n} = (n+\frac{1}{2})^2\pi^2$, it is easy to verify that for $n \geq 2$ the nth pole-strip always overlaps portions of the nth and $(n-1)$th zero-strips. Specifically, the 4th and 5th pole-strips, the 6th and 7th pole-strips, etc. resemble the 2nd and 3rd pole-strips. We can now proceed with establishing the existence of alternating imaginary poles and zeros of (38) for the general case of a fixed finite non-zero J_p^*. Without loss of generality, we treat k as a fixed parameter and examine the migration of a pole $\omega_{\mu m}$ and a zero $\omega_{\zeta n}$ as J_p^* varies in all their relevant strips (see Fig. 6). To start with, consider the first pole-strip and first zero-strip. When the first zero moves (as a result of an increased J_p^*) from $\hat{s} = j\omega_{\beta_1}$ to $\hat{s} = j\omega_{\alpha_1}$, the first pole must move from $\hat{s} = j\omega_{\alpha_1}$ to $\hat{s} = j\omega_1$ such that $\omega_{\alpha_1} > \omega_1 > 0$. As the first zero approaches $\hat{s} = j\omega_1$, the first pole approaches $\hat{s} = j\omega_2$ such that $\omega_1 > \omega_2 > 0$. Ultimately, the first zero and first pole merge into one point at $\hat{s} = 0$ as $J_p^* \to \infty$. Next, consider the second pole-strip and first zero-strip. When the second pole moves from $\hat{s} = j\omega_{\alpha_2}$ to $\hat{s} = j\omega_{\beta_1}$, the first zero must move from $\hat{s} = j\omega_{\beta_1}$ to $\hat{s} = j\omega_3$ such that $\omega_{\beta_1} > \omega_3 > 0$. If $\omega_3 > \omega_{\alpha_1}$, a further increased J_p^* will eventually bring the second pole to a point $\hat{s} = j\omega_4$ such that the first zero is located at $\hat{s} = j\omega_{\alpha 1}$, where $\omega_4 > \omega_{\gamma_1} \geq \omega_{\alpha_1}$. The case $\omega_3 \leq \omega_{\alpha_1}$ is not of concern here because it has just been discussed. Now, consider the second pole-strip and second zero-strip. When the

second zero moves from $\hat{s} = j\omega_{\beta_2}$ to $\hat{s} = j\omega_{\alpha_2}$, the second pole must move from $\hat{s} = j\omega_{\alpha_2}$ to $\hat{s} = j\omega_5$ such that $\omega_{\alpha_2} > \omega_5 > \omega_{\gamma_1}$. As J_p^* is further increased to ∞, the second zero will eventually reach to $\hat{s} = j\omega_{\delta_1}$, and the second pole must approach $\hat{s} = j\omega_{\gamma_1}$. By the same reasoning, the above results can be extended to all other pole-strips and zero-strips. A typical root locus for a finite non-zero J_p^* is shown by (b) in Fig. 6. We conclude that, with the previously defined input and output, the single-link flexible manipulator with a tip payload is minimum phase for all $m_p^* > 0$ and $J_p^* > 0$ iff $-\infty < k \leq 0.742$.

To conclude this section, a final but not least important comment is in order. Recall that the above analysis is rooted in the transfer function of an exact linear distributed model. The above necessary and sufficient is obtained via numerical solutions of the associated exact transcendental equations. The asymptotic properties of high-mode roots are used to predict the behavior of the root locus of the high-modes. Although we have used the first 6 exact roots to construct the root locus, the asymptotic properties were found to hold even for the third mode. This means that only the first three modes are vital to the determination of qualitative behavior of zeros of $G(s,k)$. It is interesting to point out that almost all control studies using finite-dimensional models to date retain two or three flexible modes in their work without justification. The above analysis suggests that at least the first

three modes of zeros are required to faithfully capture the actual behavior of a noncollocated single-link flexible manipulator system.

V. EQUIVALENCE OF THE EIGENVALUES OF ZERO-DYNAMICS AND THE ZEROS OF TRANSFER FUNCTION

In [10], the distributed parameter model of a single-link flexible manipulator without a tip payload is considered. Using $y(t,k)=\theta(t)+kv_x(\ell,t)$ as the output, the zeros of transfer function and zero-dynamics were studied separately as if they might be different. In what follows, we will establish the connection between the zeros of transfer function and the eigenvalues of zero-dynamics for our system, i.e. (8)-(13) with (15) as the output equation.

Using (10) and (8), we can write (15) and its derivatives as

$$y(t,k)=(1-k)\ell w_x(0,t)+kw(\ell,t), \tag{39}$$

$$\dot{y}(t,k)=(1-k)\ell \dot{w}_x(0,t)+k\dot{w}(\ell,t), \tag{40}$$

$$\ddot{y}(t,k)=(1-k)\frac{\ell}{I_h}[\tau(t)+EIw_{xx}(0,t)]-k\frac{EI}{\rho}w_{xxxx}(\ell,t). \tag{41}$$

Note that the relative degree of the system is always two except when $k=1$. The zero dynamics are obtained by applying a $\tau(t)$ such that $y(t,k)$, $\dot{y}(t,k)$, and

$\ddot{y}(t,k)$ are constrained to zero. Using (8), (9), (11), (12), and (39), the zero dynamics are described by

$$\rho\ddot{w}(x,t)+EIw_{xxxx}(x,t)=0, \tag{42}$$

$$w(0,t)=0, \tag{43}$$

$$(1-k)\ell w_x(0,t)+kw(\ell,t)=0, \tag{44}$$

$$m_p\ddot{w}(\ell,t)-EIw_{xxx}(\ell,t)=0, \tag{45}$$

$$J_p\ddot{w}_x(\ell,t)+EIw_{xx}(\ell,t)=0. \tag{46}$$

Our interest here is to find the eigenvalues associated with (42)-(46). The problem can be solved by the method of Laplace transform assuming zero initial conditions. Equivalently, by letting $w(x,t)=e^{st}W(x)$ and making use of (16)-(18), we obtain

$$W^{(iv)}(x)-\left(\frac{\beta}{\ell}\right)^4 W(x)=0, \tag{47}$$

$$W(0)=0, \tag{48}$$

$$(1-k)\ell W'(0)+kW(\ell)=0, \tag{49}$$

$$m_p^*\beta^4 W(\ell)+\ell W'''(\ell)=0, \tag{50}$$

$$J_p^*\beta^4 W'(\ell)-\ell^3 W''(\ell)=0. \tag{51}$$

The solution of (47) satisfying (48) can be written as

$$W(x) = A\sinh\frac{\beta}{\ell}x + B\sin\frac{\beta}{\ell}x + C(\cosh\frac{\beta}{\ell}x - \cos\frac{\beta}{\ell}x). \tag{52}$$

To further satisfy (49)-(51), we obtain

$$\begin{bmatrix} (1-k)\beta + k\sinh\beta & (1-k)\beta + k\sin\beta & k(\cosh\beta - \cos\beta) \\ m_p^*\beta\sinh\beta + \cosh\beta & m_p^*\beta\sin\beta - \cos\beta & m_p^*\beta(\cosh\beta - \cos\beta) + (\sinh\beta - \sin\beta) \\ J_p^*\beta^3\cosh\beta - \sinh\beta & J_p^*\beta^3\cos\beta + \sin\beta & J_p^*\beta^3(\sinh\beta + \sin\beta) - (\cosh\beta + \cos\beta) \end{bmatrix} \begin{bmatrix} A \\ B \\ C \end{bmatrix}$$

$$= \begin{bmatrix} 0 \\ 0 \\ 0 \end{bmatrix}. \tag{53}$$

Nontrivial solutions of (47)-(51) exist iff the determinant of the coefficient matrix in (53) vanishes. After tedious algebraic manipulation, we obtain the following characteristic equation

$$\beta K_2(\beta) + kK_3(\beta) = 0, \tag{54}$$

where $K_2(\beta)$ and $K_3(\beta)$ can be found in (21)-(22). We have thus shown the equivalence of the eigenvalues of zero-dynamics and zeros of the transfer function of the single-link flexible manipulator system described by (1)-(6) and (14). Recall that in Section 4 only the roots of (54) that correspond to pure imaginary roots in the s-plane are examined. If pure real roots in the s-plane are required, we substitute $\beta = (1+j)\sqrt{\frac{\alpha}{2}}$ into (54), where α is a real positive constant, and bear in mind that if

β is a root of (54), so are $-\beta$ and $\pm j\beta$ [2]. The roots α of the transformed characteristic equation are the type of zero-dynamics studied in [9, 10]. This explains as to why in [10] the numerator of the transfer function differs from the characteristic equation of the zero-dynamics. We conclude that the method used in [9, 10] is unable to provide the stability criterion of zero-dynamics of a system if there are unstable complex zeros in the s-plane.

IV. CONCLUSIONS

A single-link flexible manipulator having a tip payload and with noncollocated actuator and sensor has been analyzed using a linear distributed parameter model. The joint torque is considered as the input and the joint angle plus a weighted value of tip deflection is chosen as the output. A necessary and sufficient condition for the noncollocated system to be minimum phase (i.e. its transfer function does not have any zeros in the open right-half plane) has been derived. This minimum phase condition is especially valuable since it depends neither on physical parameters of the flexible link nor on the mass properties of the tip payload. The equivalence of the zeros of the transfer function and the eigenvalues of zero dynamics has also been established for the first time based on an infinite-dimensional model of the noncollocated single-link flexible manipulator system.

The result of this paper clearly provides partial justification for certain

noncollocated control designs [7, 18] based on finite-dimensional approximate models. It also broadens the scope the applicability of passivity-based PD control [19] and inversion-based trajectory tracking control [5, 20] for noncollocated single-link flexible manipulator systems. Finally, the inadequacy of the method used in [9, 10] to investigate the stability of infinite dimensional zero-dynamics is also clarifed.

Table 1. Values of ω_{zn}. ω_{pn}, $\omega_{\beta n}$, and $\omega_{\delta n}$

n	ω_{zn}	ω_{pn}	$\omega_{\beta n}$	$\omega_{\delta n}$
1	$2(2.365)^2$	1.875^2	3.927^2	4.730^2
2	$2(5.498)^2$	4.694^2	7.069^2	7.853^2
3	$2(8.639)^2$	7.855^2	10.210^2	10.996^2
4	$2(11.781)^2$	10.996^2	13.352^2	14.137^2
5	$2(14.923)^2$	14.137^2	16.493^2	17.279^2
6	$2(18.064)^2$	17.279^2	19.635^2	20.420^2
≥ 5	$2(n-\frac{1}{4})^2\pi^2$	$(n-\frac{1}{2})^2\pi^2$	$(n+\frac{1}{4})^2\pi^2$	$(n+\frac{1}{2})^2\pi^2$

Table 2. Values of $\omega_{\alpha n}(k)$

k	ω_{α_1}	ω_{α_2}	ω_{α_3}	ω_{α_4}	ω_{α_5}	ω_{α_6}
-100	0.573^2	4.900^2	7.726^2	11.085^2	14.067^2	17.336^2
-10	1.001^2	4.881^2	7.737^2	11.078^2	14.073^2	17.331^2
-1	1.551^2	4.798^2	7.791^2	11.041^2	14.102^2	17.308^2
-0.7	1.620^2	4.780^2	7.802^2	11.033^2	14.108^2	17.303^2
-0.5	1.676^2	4.764^2	7.812^2	11.026^2	14.114^2	17.298^2
-0.3	1.742^2	4.743^2	7.825^2	11.016^2	14.121^2	17.292^2
0	1.875^2	4.694^2	7.855^2	10.996^2	14.137^2	17.279^2
0.3	2.082^2	4.601^2	7.909^2	10.956^2	14.167^2	17.254^2
0.5	2.318^2	4.468^2	7.980^2	10.904^2	14.208^2	17.221^2
0.7	2.847^2	4.082^2	8.145^2	10.777^2	14.301^2	17.142^2
0.730	3.029^2	3.927^2	8.191^2	10.741^2	14.327^2	17.120^2
0.742	3.142^2	3.825^2	8.213^2	10.724^2	14.339^2	17.110^2
0.758	3.491^2	3.491^2	8.245^2	10.698^2	14.357^2	17.094^2

Table 3. Values of $\omega_{\gamma n}(k)$

k	ω_{γ_1}	ω_{γ_2}	ω_{γ_3}	ω_{γ_4}	ω_{γ_5}	ω_{γ_6}
-100	1.962^2	5.622^2	8.557^2	11.840^2	14.875^2	18.103^2
-10	2.003^2	5.612^2	8.564^2	11.835^2	14.879^2	18.100^2
-1	2.183^2	5.561^2	8.598^2	11.811^2	41.899^2	18.084^2
-0.7	2.217^2	5.550^2	8.606^2	11.806^2	14.903^2	18.080^2
-0.5	2.247^2	5.540^2	8.612^2	11.801^2	14907^2	18.077^2
-0.3	2.285^2	5.527^2	8.620^2	11.795^2	14.912^2	18.073^2
0	2.365^2	5.498^2	8.639^2	11.781^2	14.923^2	18.064^2
0.3	2.501^2	5.442^2	8.674^2	11.755^2	14.943^2	18.047^2
0.5	2.665^2	5.366^2	8.721^2	11.721^2	14.970^2	18.025^2
0.7	3.001^2	5.175^2	8.827^2	11.639^2	15.033^2	17.972^2
0.730	3.098^2	5.117^2	8.857^2	11.616^2	15.050^2	17.957^2
0.742	3.142^2	5.088^2	8.871^2	11.604^2	15.058^2	17.950^2
0.758	3.205^2	5.044^2	8.892^2	11.588^2	15.070^2	17.940^2

APPENDIX

The infinite product expansions for transcendental functions used in this paper are summarized as follows [16, 2]. In accordance with the context of this paper, $\hat{s}^2 = -\beta^4$ is used whenever it is appropriate.

A1. $\sinh\beta + \sin\beta = 2\beta\prod_{n=1}^{\infty}(1-\frac{\hat{s}^2}{\omega_{zn}^2}), \qquad \omega_{zn} = 2a_n^2$

$\tanh a_n + \tan a_n = 0, \qquad (a_n > 0, \text{ real}).$

$a_n = (n-\frac{1}{4})\pi \quad \text{as} \quad n \to \infty.$

A2. $1+\cosh\beta\cos\beta = 2\prod_{n=1}^{\infty}(1+\frac{\hat{s}^2}{\omega_{pn}^2}), \qquad \omega_{pn} = b_n^2.$

$\cosh b_n \cos b_n + 1 = 0, \qquad (b_n > 0, \text{ real}).$

$b_n = (n-\frac{1}{2})\pi \quad \text{as} \quad n \to \infty.$

A3. $\cos\beta\sinh\beta - \sin\beta\cosh\beta = -\frac{2}{3}\beta^3\prod_{n=1}^{\infty}(1+\frac{\hat{s}^2}{\omega_{\beta n}^2}), \qquad \omega_{\beta n} = c_n^2.$

$\tanh c_n - \tan c_n = 0, \qquad (c_n > 0, \text{ real}).$

$c_n = (n+\frac{1}{4})\pi \quad \text{as} \quad n \to \infty.$

A4. $\cosh\beta\sin\beta + \sinh\beta\cos\beta = 2\beta\prod_{n=1}^{\infty}(1+\frac{\hat{s}^2}{\omega_{zn}^2}), \qquad \omega_{zn} = a_n^2.$

$\tanh a_n + \tan a_n = 0, \qquad (a_n > 0, \text{ real}).$

$a_n = (n-\frac{1}{4})\pi \quad \text{as} \quad n \to \infty.$

A5. $\cosh\beta - \cos\beta = \beta^2 \prod_{n=1}^{\infty} (1 - \frac{\hat{s}^2}{4n^4\pi^4})$.

A6. $1 - \cosh\beta\cos\beta = -\frac{1}{6}\hat{s}^2 \prod_{n=1}^{\infty}(1 + \frac{\hat{s}^2}{\omega_{\delta n}^2})$, $\omega_{\delta n} = d_n^2$.

$\cosh d_n \cos d_n - 1 = 0$ ($d_n > 0$, real).

$d_n = (n + \frac{1}{2})\pi$ as $n \to \infty$.

Note that the asymptotic expressions are quite accurate for $n \geq 5$.

REFERENCES

1. Cannon, R.H. Jr. and E. Schmitz, "Initial Experiments on the End-Point Control of a Flexible One-Line Robot," *Int. J. Robotics Research*, Vol.3, pp. 62-75 (1984).

2. Spector, V.A. and H. Flashner, "Modeling and Design Implications of Noncollocated Control in Flexible systems," *ASME J. Dyn. Syst. Meas. Contr.*, Vol. 112, pp. 186-193 (1990).

3. Park, J.H. and H. Asada, "Dynamic Analysis of Noncollocated Flexible Arms and Design of Torque Transmission Mechanisms," *ASME J. Dyn. Syst. Meas. Contr.*, Vol. 116, pp. 201-207 (1994).

4. De Luca, A. and L. Lanari, "Achieving Minimum Phase Behavior in a One-Link Flexible Arm," *Proc. Int. Symp. on Intelligent Robotics*, Bangalore, India, pp. 224-235 (1991).

5. De Luca, A., P. Lucibello, and G. Ulivi, "Inversion Techniques for Trajectory Control of Flexible Robot Arms," *J. Rob. Syst.*, Vol. 6, pp. 325-344 (1989).

6. De Luca, A., "Zero Dynamics in Robotic Systems," in Nonlinear synthesis (C.I. Byrnes and A. Kurzhansky, Eds.), Birkhauser, Boston, pp. 68-87 (1991).

7. Madhavan, S.K., and S.N. Singh, "Inverse Trajectory Control and Zero Dynamics Sensitivity of an Elastic Manipulator," *Proc. 1991 American contr.*

Conf., Boston, MA., pp. 1879-1884 (1991).

8. Wang, D. and M. Vidyasagar, "Transfer Function for a Single Flexible Link," *Int. J. Robot. Res.*, Vol. 10, pp. 540-549 (1991).
9. Tarn, T.J., C. Guo and A.K. Bejczy, "Issues in the Zeros of Flexible Robot Systems," *Proc. 32nd Allerton Conf. on Communication, Control and Computing,* pp. 641-650 (1994).
10. Chodavarapu, P.A. and M.W. Spong, "On Noncollocated Control of a Single Flexible Link," *Proc. IEEE Int. Conf. on Rob. Autom.*, Minneapolis, Minnesota, pp. 1101-1106 (1996).
11. Marino, R. and P. Tomei, Nonlinear Control Design: Geometric, Adaptive, and Robust, Prentice Hall, Europe, pp. 152-153 (1995).
12. Lee, S. and J.L. Junkins, "Explicit Generalization of Lagrange's Equations for Hybrid Coordinate Dynamical systems," *J. Guid., Contr., and Dyn.*, Vol. 15, pp. 1443-1452 (1992).
13. Wang, F.Y. and G. Guan, "Influences of Rotatory Inertia, Shear and Loading on Vibrations of Flexible Manipulations," *J. of Sound and Vibration*, Vol. 171, pp. 433-452 (1994).
14. Low, K.H. and M.W. S. Lau, "Experimental Investigation of Boundary Condition of Slewing Beams Using a High-Speed Camera system," *Mechanism and Machine Theory*, Vol. 30, pp. 629-643 (1995)

15. Low, K.H., "A Note on the Effect of Hub Inertia and Payload on the Vibration of a Flexible Slewing Link," *J. of Sound and Vibration*, Vol. 204, pp. 823-828 (1997).

16. Goodson, R.E., "Distributed System Simulation Using Infinite Product Expansions," *Simulation*, pp. 255-263 (1970).

17. Jeffreys, H. and B.S. Jeffreys, Method of Mathematical Physics, 2nd Edition, Combrige University Press, Cambrige, pp. 383-386 (1950).

18. Yim, W. and S.N. Singh, "Sliding Mode Force, Motion Control, and Stabilization of Elastic Manipulator in the Presence of Uncertainties," *J. of Rob. Syst.*, Vol. 12, pp. 315-330, pp. 383-386 (1992).

19. Wang, D. and M. Vidyasagar, "Passive Control of a Stiff Flexible Link," *Int. J. Robotic Research*, Vol. 11, pp. 572-578 (1992).

20. Yim, W. and S.N. Singh, "Inverse Force and Motion Control of Constrained Elastic Robots," *ASME J. Dyn. Meas. Contr.*, Vol. 117, pp. 374-383 (1995).

CAPTIONS FOR FIGURES

Fig. 1. Schematic of the single-link flexible manipulator.

Fig. 2. Root locus of (28) for $-\infty < k < 1$ using 6 pole-zero pair approximation $(m_p^* = 0,\ J_p^* = 0)$.

Fig. 3. Root locus of (31) for $0 < m_p^* < \infty$, $J_p^* = 0$.

Fig. 4. Root locus of (34) for $0 < J_p^* < \infty$, $m_p^* = 0$.

Fig. 5. Root locus of (37).

Fig. 6. Root locus of (38) for $0 < m_p^* < \infty$.

(a) $J_p^* = 0$, (b) $0 < J_p^* < \infty$, (c) $J_p^* = \infty$.

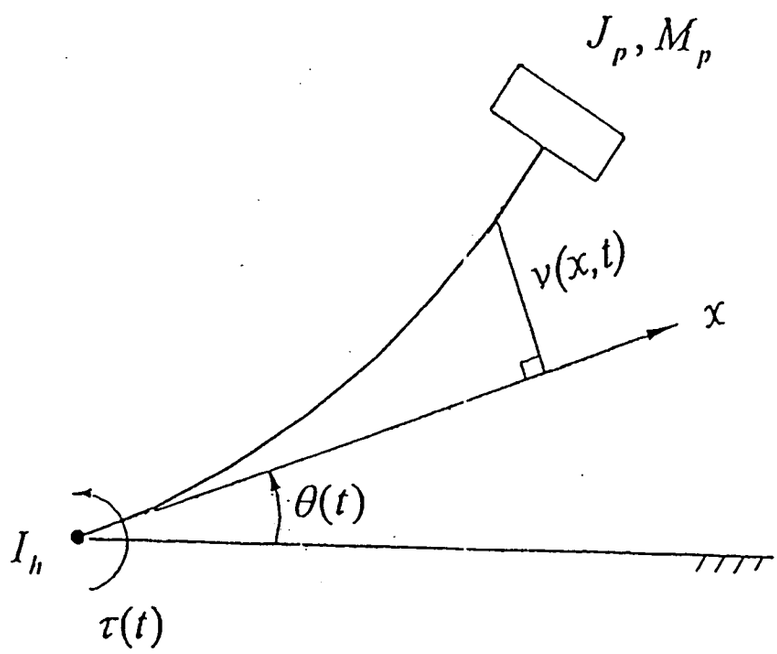

Fig. 1. Schematic of the single-link flexible manipulator.

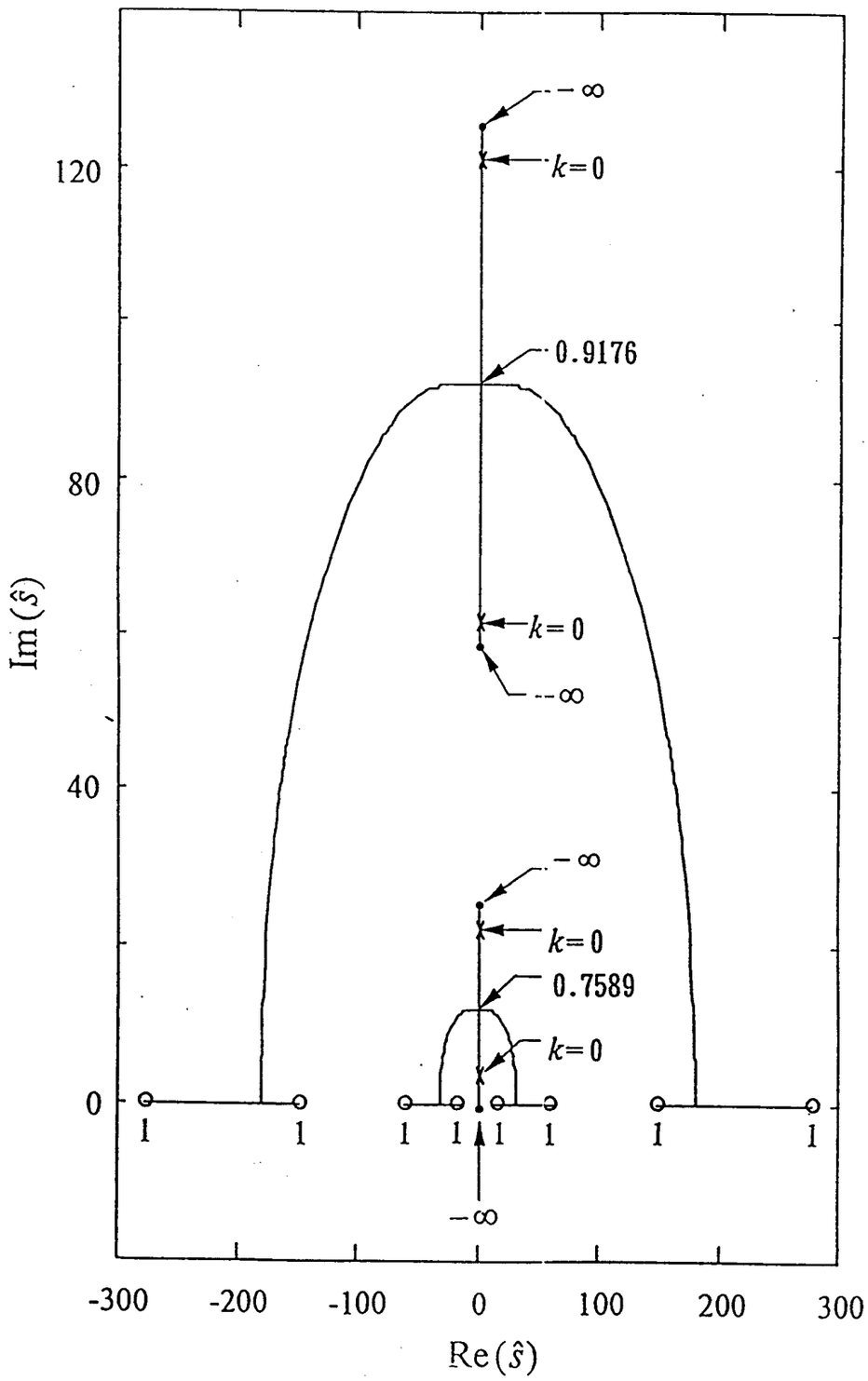

Fig. 2. Root locus of (28) for $-\infty < k < 1$ using 6 pole-zero pair approximation $(m_p^* = 0,\ J_p^* = 0)$.

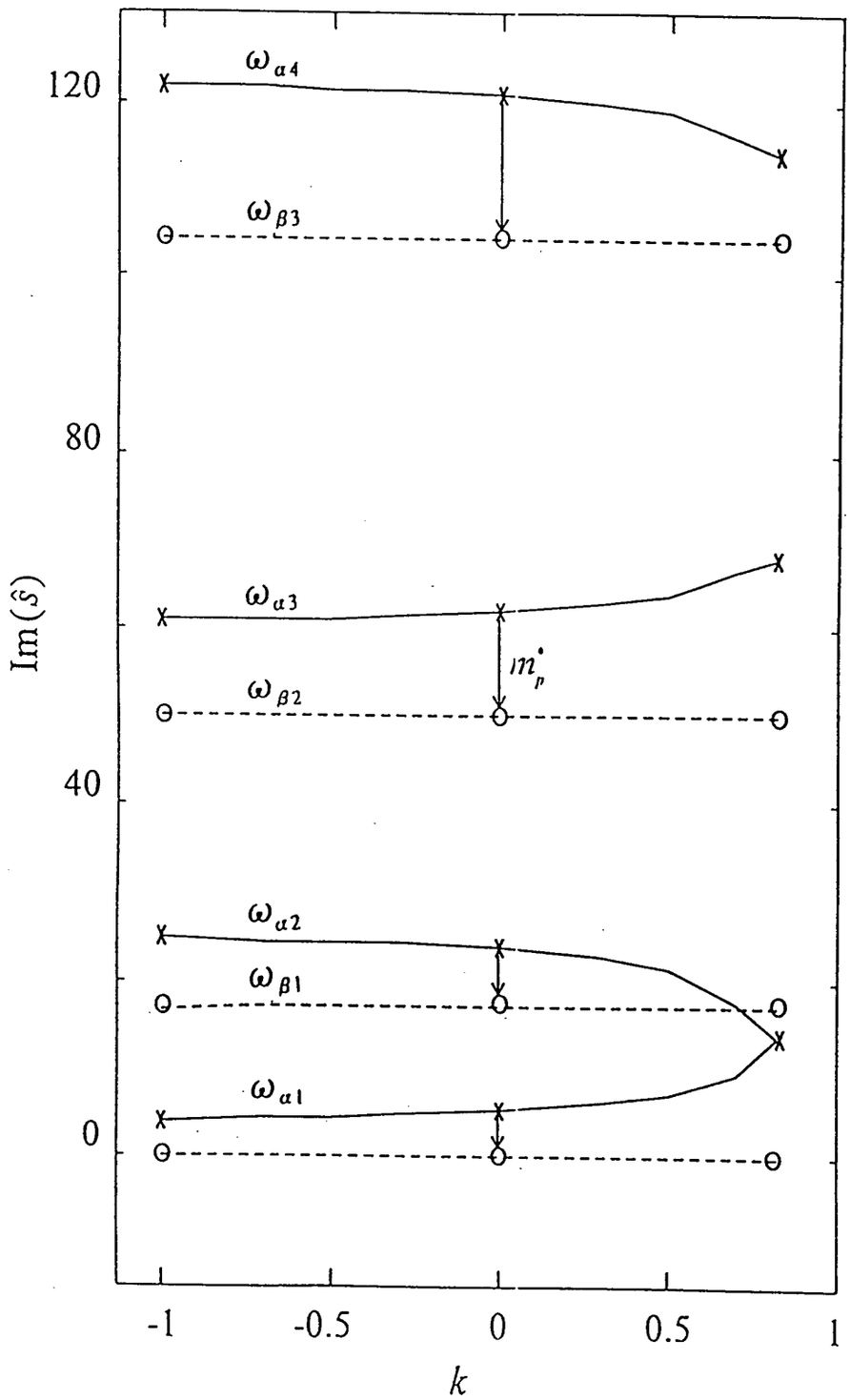

Fig. 3. Root locus of (31) for $0 < m_p^* < \infty$, $J_p^* = 0$.

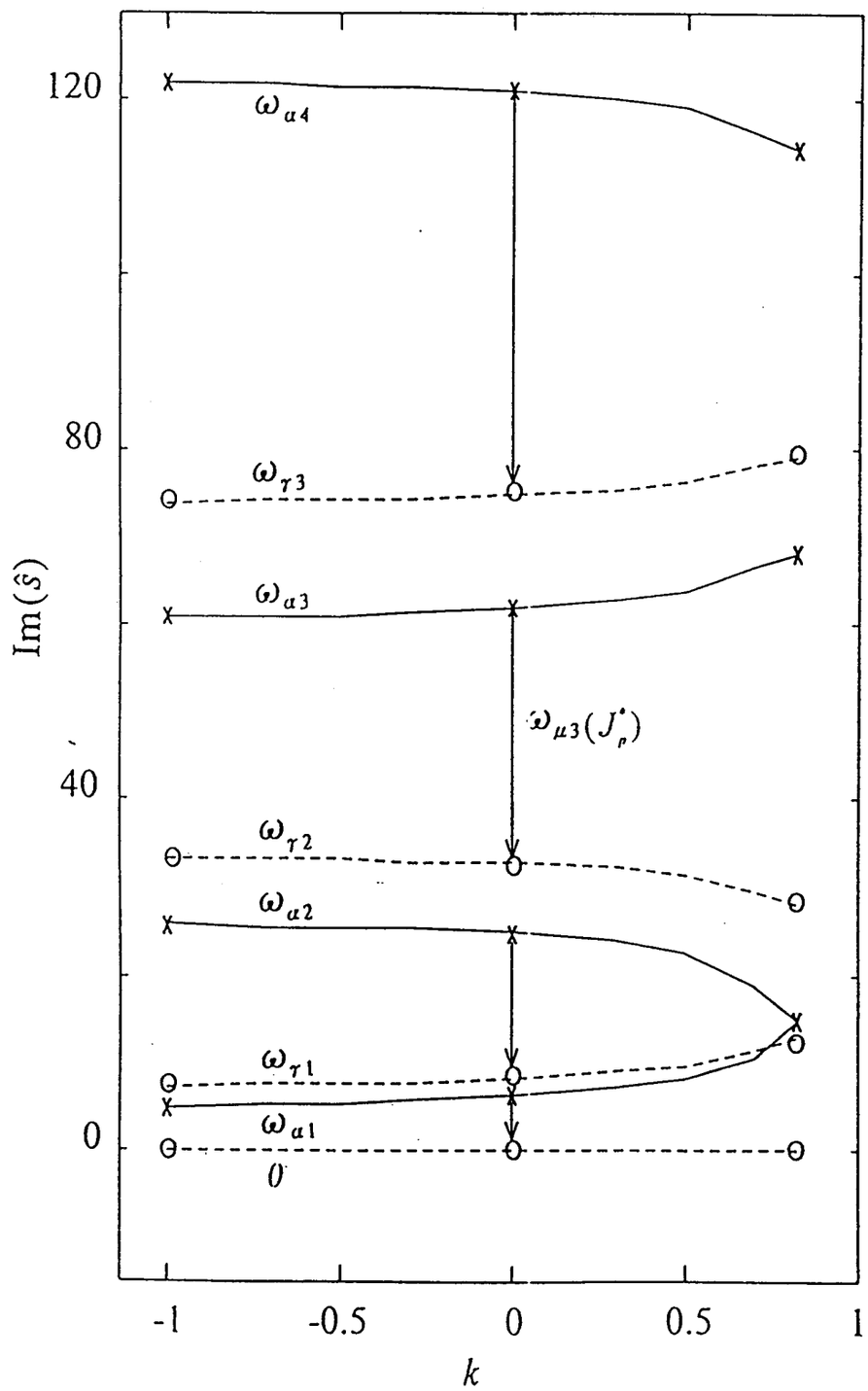

Fig. 4. Root locus of (34) for $0 < J_p^* < \infty$, $m_p^* = 0$.

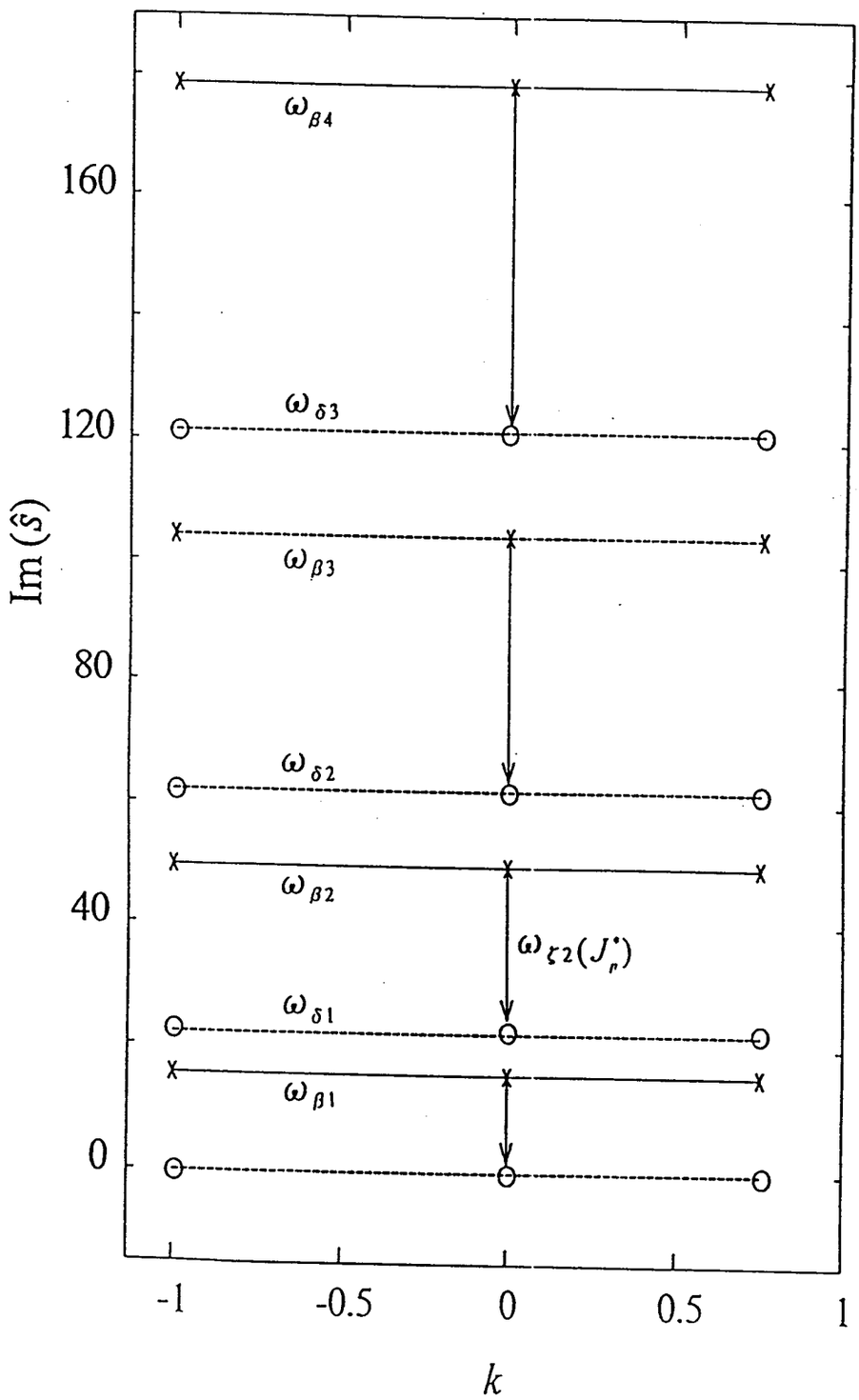

Fig. 5. Root locus of (37).

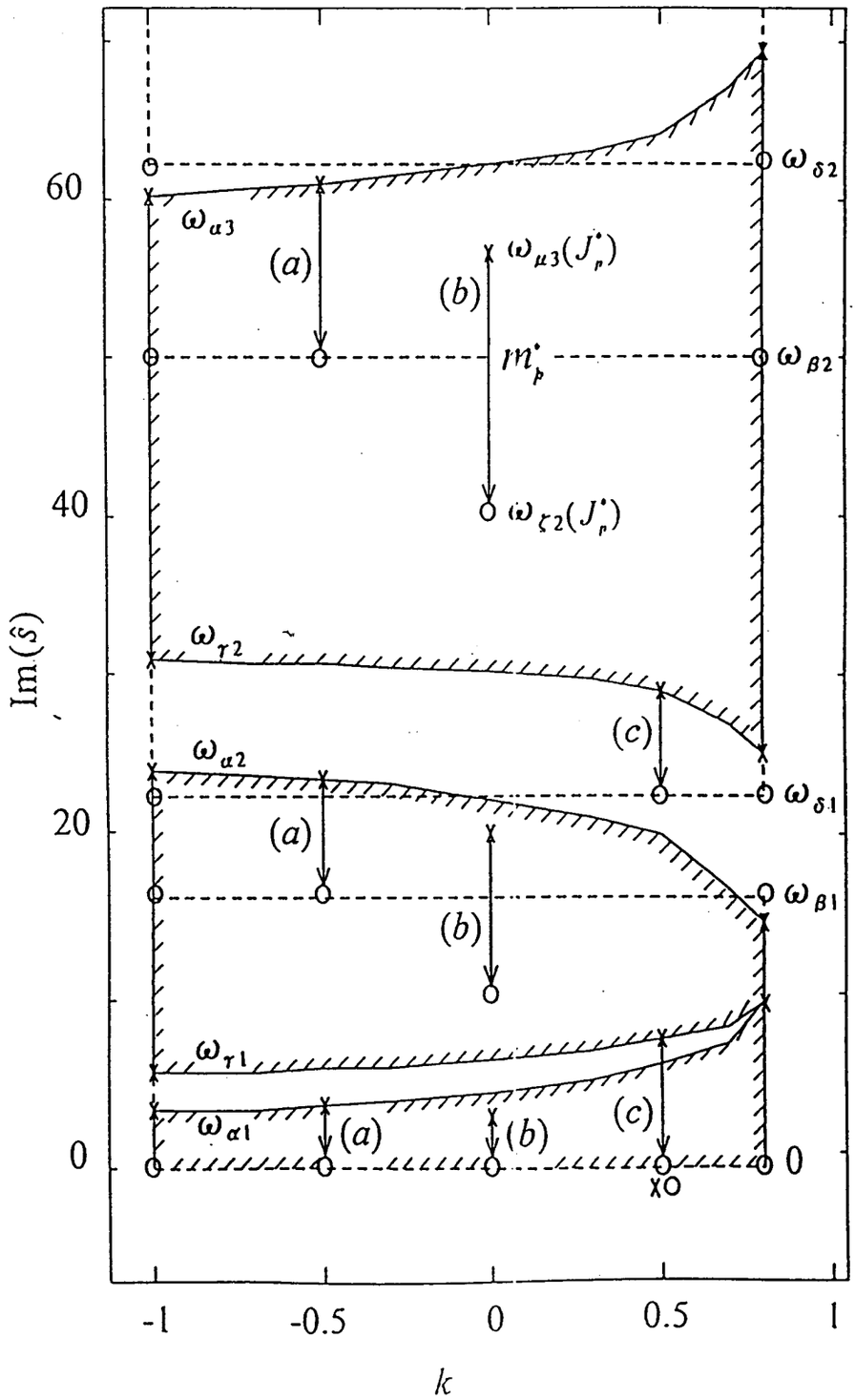

Fig. 6. Root locus of (38) for $0 < m_p^* < \infty$. (a) $J_p^* = 0$, (b) $0 < J_p^* < \infty$, (c) $J_p^* = \infty$.